View metadata, citation and similar papers at core.ac.uk
brought to you by CORE
provided by KU ScholarWorks

Molecular Biology of the Cell
Vol. 9, 3505–3519, December 1998

Drosophila coracle, a Member of the Protein 4.1 Superfamily, Has Essential Structural Functions in the Septate Junctions and Developmental Functions in Embryonic and Adult Epithelial Cells

Rebecca S. Lamb,*† Robert E. Ward,* Liang Schweizer,‡ and Richard G. Fehon§

Developmental, Cellular, and Molecular Biology Group, Duke University, Durham, North Carolina 27708-1000

Submitted May 1, 1998; Accepted September 15, 1998
Monitoring Editor: Judith Kimble

Although extensively studied biochemically, members of the Protein 4.1 superfamily have not been as well characterized genetically. Studies of *coracle*, a *Drosophila* Protein 4.1 homologue, provide an opportunity to examine the genetic functions of this gene family. *coracle* was originally identified as a dominant suppressor of $Egfr^{Elp}$, a hypermorphic form of the *Drosophila Epidermal growth factor receptor* gene. In this article, we present a phenotypic analysis of *coracle*, one of the first for a member of the Protein 4.1 superfamily. Screens for new *coracle* alleles confirm the null *coracle* phenotype of embryonic lethality and failure in dorsal closure, and they identify additional defects in the embryonic epidermis and salivary glands. Hypomorphic *coracle* alleles reveal functions in many imaginal tissues. Analysis of *coracle* mutant cells indicates that Coracle is a necessary structural component of the septate junction required for the maintenance of the transepithelial barrier but is not necessary for apical–basal polarity, epithelial integrity, or cytoskeletal integrity. In addition, *coracle* phenotypes suggest a specific role in cell signaling events. Finally, complementation analysis provides information regarding the functional organization of Coracle and possibly other Protein 4.1 superfamily members. These studies provide insights into a range of in vivo functions for *coracle* in developing embryos and adults.

INTRODUCTION

The Protein 4.1 gene superfamily consists of a functionally diverse group of proteins that nonetheless share highly conserved structural features. Members of this family include Protein 4.1, *Drosophila* Coracle, Merlin (the protein product of the *Neurofibromatosis 2* [*NF2*] gene), the Ezrin, Radixin, and Moesin (ERM) proteins, talin, *Drosophila* Expanded, several protein tyrosine phosphatases, and others (Rees *et al.*, 1990; McCartney and Fehon, 1997). All contain a functional domain of 200–300 aa that is typically found in the N-terminal half of the protein and is thought to interact with the cytoplasmic domain of particular transmembrane proteins, thereby localizing the protein to the cytoplasmic face of the plasma membrane (Rees *et al.*, 1990). In addition, Protein 4.1 contains within this region sites for interaction with p55 (Alloisio *et al.*, 1993) and hDLG (Lue *et al.*, 1994), members of the membrane-associated guanylate kinase homologues family of proteins, which also interact with the cytoplasmic tail of transmembrane proteins. Some members of the Protein 4.1 and membrane-associated guanlylate kinase homologues superfamilies are found at intercellular junctions, the primary sites of cell–cell contact and cellular communication (Fehon *et*

* These authors contributed equally to this work.
Present addresses: †Department of Molecular, Cellular, and Developmental Biology, Yale University, New Haven, CT 06520; ‡ Zoologishes Institute, Universität Zürich-Irchel, Zürich CH-8057, Switzerland.
§ Corresponding author. E-mail address: rfehon@duke.edu.

© 1998 by The American Society for Cell Biology

al., 1997; Ponting *et al.*, 1997). Recent work, in particular the identification of the *NF 2* tumor suppressor gene as a member of this family (Rouleau *et al.*, 1993; Trofatter *et al.*, 1993), has generated considerable interest in possible functions of these proteins in mediating cellular interactions that occur within the junctional complex.

Although most functional data regarding Protein 4.1 family members are based on biochemical studies of the proteins they encode, limited genetic data on some of these genes are also available. In humans, loss of *Merlin* function results in the bilateral schwannomas and other benign tumors that characterize the NF2 disease (Martuza and Eldridge, 1988). Homozygous mutant mice in which this gene has been "knocked out" fail to survive to the point of embryonic gastrulation and have defects in the extra-embryonic tissues (McClatchey *et al.*, 1997). *Protein 4.1* mutations in humans have been associated with hemolytic anemias, but although this protein is widely expressed, defects in other tissues have not been reported (Conboy *et al.*, 1993). Injection of Protein 4.1 antisense oligonucleotides into *Xenopus* embryos results in various defects, including retinal degeneration and abnormal body size (Giebelhaus *et al.*, 1988). In addition, studies of *Drosophila expanded*, a divergent member of this superfamily, indicate that like the *NF2* gene, *expanded* seems to be necessary to restrict cellular proliferation (Boedigheimer and Laughon, 1993; Boedigheimer *et al.*, 1993). However, with the exception of *expanded*, none of these genes has been studied in a system that is amenable to mutagenesis and phenotypic characterization.

To better understand the in vivo functions of these proteins, we have initiated a molecular–genetic analysis of *coracle*, a *Drosophila* homologue of Protein 4.1. Severe *coracle* mutations result in a failure of dorsal closure and lethality late in the process of embryonic development (Fehon *et al.*, 1994). Confocal and immunoelectron microscopy using specific antibodies have shown that Coracle localizes to septate junctions, a primary site of cell–cell contact and growth regulation in *Drosophila* epithelial cells. Other proteins known to be associated with this junctional region include the products of the *discs large* (*dlg*) (Woods and Bryant, 1989) and *Neurexin* (*Nrx*) (Baumgartner *et al.*, 1996) genes. Mutations in *dlg* result in disrupted apical–basal cellular polarity and overgrowth in the imaginal epithelia (Abbott and Natzle, 1992; Woods *et al.*, 1997), whereas mutations in *Nrx* show dorsal closure defects and disruption of the blood–brain barrier (Baumgartner *et al.*, 1996). In addition, *coracle* mutations dominantly suppress eye phenotypes associated with the $Egfr^{EIP}$ mutation, a gain of function mutation in *Egfr* (Baker and Rubin, 1992; Fehon *et al.*, 1994). Mutations in *Egfr* have been shown to affect cell proliferation in imaginal discs (Diaz-Benjumea and Garcia-Bellido, 1990; Xu and Rubin, 1993). Together, these results implicate the septate junction in mediating cellular interactions necessary for normal growth control in *Drosophila* epithelia.

We present here the results of screens for new *coracle* alleles, and their embryonic and adult phenotypes. One advantage of such an approach is that is does not require previous knowledge of the functions of a particular gene, nor do such notions bias it if they do exist. Our results indicate that *coracle* provides essential functions throughout development in various epithelia, including the embryonic epidermis and salivary glands, and adult structures such as the eyes, wings, ocelli, and other tissues. We provide evidence that *coracle* function is required for the maintenance of the transepithelial barrier function of the septate junction and suggest that this role of the septate junction is crucial for the establishment of a unique apical environment. Interestingly, despite its structural similarity to a vertebrate cytoskeletal protein and its localization to a major component of the apical junctional complex, Coracle does not appear to be required for epithelial integrity, apical–basal polarity, or organization of the actin cytoskeleton.

MATERIALS AND METHODS

Isolation of coracle Alleles

The *coracle* alleles used in this study were generated in three independent genetic screens. cor^1 and cor^2 were isolated and characterized previously (Fehon *et al.*, 1994). Further alleles were isolated in an F_2 lethal screen. *cn*; ry^{506} males were mutagenized with methane–sulfonic acid ethyl ester and mated to *y w*; *Sco/CyO* females according to standard procedures (Grigliatti, 1986). F_1 males were individually mated to *y w*; cor^2 *px sp/CyO* females, and the resulting F_2 progeny were screened for lethality over the cor^2 *px sp* chromosome. Fertile F_1 crosses (10,046) were screened, and 12 independent alleles, cor^3–cor^{14}, were recovered. All chromosomes were "cleaned" by recombination of flanking markers. Except where noted in Table 1, all lines are rescuable in homozygous condition by a *Ubiquitin*-promoter–driven cor^+ cDNA transgene, $P\{w^{+mc}$, *Up-*$cor^+ = cor^+\}$, which we abbreviate as the $P\{Up\text{-}cor^+\}$ transgene (Fehon *et al.*, 1994).

cor^{15} was isolated in a separate F_1 visible screen. *cn*; ry^{506} males were mutagenized with methane–sulfonic acid ethyl ester and mated to cor^2 *px sp/CyO* females according to standard procedures (Grigliatti, 1986). The resulting F_1 progeny were screened for males in which a visible phenotype in the eye or other cuticular structures were evident over cor^2 *px sp*. F_1 males (24,590) were screened, and 214 individuals were selected. Individuals that bred true and segregated with the second chromosome were retained for further analysis. In this screen one allele, cor^{15}, was isolated.

Complementation Analysis

We performed pairwise crosses between all *coracle* alleles plus two deficiencies that uncover the *coracle* locus. Crosses were performed in duplicate at 18 and 25°. Embryos were collected on apple juice agar plates as described (Wieschaus *et al.*, 1984). A total of 250 embryos per cross were followed, and the level of embryonic lethality was determined. Larvae that crawled away were transferred to vials, and the number of larvae that pupariated was determined. Finally, the number of adults that eclosed was counted. Sufficient numbers of offspring were examined so that at least 200 *coracle*

mutant offspring would be expected if the allelic combination was viable. Mutant viability was calculated by dividing the number of mutant flies by the number of balancer class siblings that eclosed. Surviving *coracle* hypomorphs were examined for phenotypes. Scanning electron microscopy was performed on a Philips model 501 microscope (FEI Company, Hillsboro, OR) as described previously (Rebay *et al.*, 1993). Fertility of the *coracle* hypomorphs was examined by crossing one to five cor^x/cor^y males and females to w^{1118} females and males, respectively, and examining vials for viable offspring.

Cuticle Preparations

Cuticle preparations were performed as described (Szüts *et al.*, 1997) with the following modifications. The cuticles were expanded in 1× PBS, 0.1% Triton X-100 for 20 min at 65°C, and then allowed to settle overnight at room temperature through diluted Hoyer's solution (2:1:1, Hoyer's:lactic acid:ddH_2O). Cuticles were then mounted in diluted Hoyer's solution and allowed to clear for several days.

Transmission Electron Microscopy

Fixation of embryos for transmission electron microscopy was performed as described (Tepass and Hartenstein, 1994) with the following modifications. After the devitellinization step, the late stage 17 embryos were bisected midway between the anterior and posterior ends. Additionally, the electron microscopy fixation and osmication steps were doubled in length to 4 and 2 h, respectively. A subset of embryos was devitellinized with methanol to investigate the cuticular phenotype, which was more apparent under these conditions. Sections (30–80 nm) were cut on an AO/Reichert Ultracut ultramicrotome (American Optical Scientific Instruments, Buffalo, NY) and were analyzed on a Zeiss EM 10A electron microscope (Carl Zeiss, Oberkochen, West Germany).

Dye Permeability Experiments

Progeny from a cross of *cor*^{5}*/CyO, P{w*$^+$*; hsMerlinGFP}* were collected for 1 h, aged for 10–12 h, and then heat-shocked for 1 h at 38°C to induce the expression of the *Merlin-GFP* transgene in all heterozygous and homozygous balancer class embryos. The embryos were subsequently aged 3–4 h and then dechorionated in 50% commercial bleach (12% sodium hypochlorite). The embryos were arrayed on apple juice plates, transferred to double-stick tape on glass coverslips, and desiccated in a closed container containing Drierite (W. A. Hammond Drierite Company, Xenia, OH) for 20 min. The embryos were then covered with halocarbon oil (Halocarbon, North Augusta, SC). Rhodamine-labeled dextran (M_r, 10,000; Molecular Probes, Eugene, OR) in injection buffer (Rubin and Spradling, 1982) was then injected into the hemocoel using a micromanipulator under a microscope, and the embryos were examined on a Zeiss LSM 410 laser scanning confocal microscope with a krypton/argon laser (Carl Zeiss, Thornwood, NY).

Genetic Interactions with Egfr

Ten cor^x/CyO males were mated to 20 $Egfr^{Elp}/CyO$ virgin females, and the $cor^x/Egfr^{Elp}$ offspring were examined for suppression of the $Egfr^{Elp}/+$ dominant rough eye phenotype. Crosses were performed at 25°C. Specimens were prepared for scanning electron microscopy on a Philips model 501 microscope (FEI Company, Hillsboro, OR) as described previously (Rebay *et al.*, 1993).

Clonal Analysis

The *cor*^{4} allele was crossed onto an FRT43D chromosome (Xu and Rubin, 1993). w^{1118}, *hsFLP*; *FRT43D P{y*$^+$*}* virgin females were mated to *y w*; *FRT43D cor*^{4}*/CyO* males. Mitotic clones were induced 76 h after egg laying by two 1-h heat shocks at 38°C separated by a 1-h 25°C recovery and examined in late third instar imaginal discs.

Immunofluorescence

Embryos aged 0–14 h were collected from *y w*; *FRT43D cor*^{5}*/CyO* adults and fixed and stained as described previously (Fehon *et al.*, 1991). Third instar wing imaginal discs were dissected, fixed, and stained as described previously (Fehon *et al.*, 1994). Primary antibodies were used at the following dilutions: guinea pig anti-Coracle, 1:10,000 (embryos) or 1:5000 (discs); mouse anti-Neurexin, 1:1000; mouse anti-Notch (C17.9C6), 1:3000; rabbit anti-Armadillo (gift from M. Peifer, University of North Carolina, Chapel Hill, NC), 1:500; mouse anti-Crumbs (gift from E. Knust, Universität Düsseldorf, Düsseldorf, Germany), 1:100; rabbit anti–β_H-Spectrin (gift from G. Thomas, Pennsylvania State University, University Park, PA), 1:2000; rabbit anti–α-Spectrin (gift from D. Kiehart, Duke University, Durham, NC) 1:1000; and mouse anti-Moesin, 1:10,000. All secondary antibodies were from Jackson ImmunoResearch (West Grove, PA). Rhodamine-conjugated phalloidin (Molecular Probes) was added with the primary antibody at a dilution of 1:1000.

RESULTS

Isolation of coracle *Point Mutations and Deficiencies*

The *coracle* gene was simultaneously identified as a *Drosophila* Protein 4.1 homologue and in a screen for dominant suppressors of the rough eye phenotype caused by $Egfr^{Elp}$ (Fehon *et al.*, 1994). Initial phenotypic analysis of two alleles, *cor*^{1} and *cor*^{2}, indicated that *coracle* has an essential role during embryonic dorsal closure. However, the limited number of alleles and the lack of an existing deficiency with which to examine the null phenotype limited our ability to thoroughly examine *coracle* phenotypes in embryonic and adult development. To better understand the functions of *coracle*, we have conducted genetic screens for new *coracle* alleles, resulting in the identification of 13 new *coracle* mutations (Table 1).

To aid in the characterization of these alleles, we have also identified two small deficiencies that uncover *coracle*. One was originally identified as a gamma ray-induced allele of *enabled*, $Df(2R)enb^{GC8}$, which had been mapped to the 56A-F interval (Konsolaki and Schupbach, 1998). The second deficiency, $Df(2R)cor^{P97}$, was induced by imprecise excision of *P{white-un3}AA48* in region 56B (B. McCartney and R. Fehon, unpublished data). Both of these deficiencies fail to complement the *cor*^{1} and *cor*^{2} point mutations (as well as *enb* point mutations), and quantitative hybridization analysis using a *coracle* cDNA probe shows that both deficiencies remove all *coracle* coding sequences (our unpublished results). Thus, these deficiencies are useful for determining the null *coracle* phenotype and the genetic function of *coracle* point mutations.

Classification of coracle Alleles

To assess its severity, each of the *coracle* alleles was examined in homozygous condition and in *trans* with $Df(2R)cor^{P97}$. We then ranked these alleles into three classes, strong, intermediate, and weak, on the basis of

Table 1. Summary of *coracle* alleles

Allele	Lethal period	Embryonic phenotype[a]	Adult escapers	*P{Up-cor$^+$}* rescue?	Phenotypic category[b]	*Egfr^{Elp}* suppression
cor^1	E	DS/FC	N	Y	I	+++
cor^2	E	DH/FC	N	Y	S	+++
cor^3	E	DH/FC	N	Y	S	+
cor^4	E	DH/FC	N	Y	S	++
cor^5	E	DH/FC	N	Y	S	++
cor^6	E	AO/DH/FC	N	P	S	++
cor^7	E/L	FC	Y	Y	I	+/++
cor^8	E/L	FC	Y	P	W	+
cor^9	E/L	FC	N	N	W	N
cor^{10}	E/L	FC	Y	Y	W	+
cor^{11}	E/L	FC	N	N	W	N
cor^{12}	E	DS/FC	N	Y	I	++++
cor^{13}	E	DS/FC	N	Y	I	+++
cor^{14}	L	N	Y	Y	W	++
cor^{15}	N	N	Y	Y	W	++++

[a] Abbreviations: DS, dorsal scab; DH, dorsal hole; AO, anterior open; FC, faint cuticle; E, embryo; L, larva; N, none; Y, yes; P, partial; I, intermediate; S, strong; W, weak; ++++, eye appears wild-type; +++, eye is wild-type in size with some roughening; ++, eye is smaller than wild-type with some roughening; +, eye is less rough than an *Egfr^{Elp}* eye in a wild-type background.

[b] See text for explanation of categories.

the severity of embryonic phenotype when in *trans* with *Df(2R)cor^{P97}* (Table 1). Strong alleles are characterized by moderately to highly penetrant dorsal defects (dorsal hole or scab) (Figure 1, B and G), whereas intermediate alleles are embryonic lethal but only rarely display dorsal defects. Weak alleles are either embryonic or larval lethal and show no dorsal defects. Two alleles, *cor^{14}* and *cor^{15}*, show no embryonic lethality when homozygous or in *trans* with the deficiency and are classified as weak alleles. Most strong and all intermediate alleles show a greater penetrance of the dorsal closure phenotype when in *trans* with *Df(2R)cor^{P97}* than when homozygous, indicating that the dorsal closure defect represents the null phenotype for the *coracle* locus. Only one allele, *cor^5*, displays a consistently strong dorsal closure phenotype in either condition. *cor^5* mutant embryos also fail to express any detectable Coracle protein (Figure 2B), whereas all other alleles express detectable amounts of Coracle (our unpublished results). We therefore conclude that *cor^5* is a null allele.

One allele, *cor^6*, is unusual in that it displays a highly penetrant anterior open phenotype in homozygous condition (Figure 1H), whereas when placed in *trans* over a deficiency it displays a characteristic dorsal closure phenotype (Figure 1G). This result indicates that either the *cor^6* chromosome carries a second site mutation that is epistatic to *coracle* or that the *cor^6* mutation conveys a neomorphic or possibly antimorphic function on the *coracle* gene. In support of the latter notion, we find that *cor^6* is rescuable in a dose-dependent manner by the *P{Up-cor$^+$}* transgene (Fehon *et al.*, 1994), although this rescue is incomplete (Table 1). One dose of *P{Up-cor$^+$}* rescues 11% of the expected progeny, whereas two doses of the transgene rescue 29% of the expected progeny. By contrast, one dose of the *P{Up-cor$^+$}* transgene rescues 96% of the expected *cor^5* homozygotes. In addition, the viability of *cor^6*/+ heterozygotes is enhanced by *P{Up-cor$^+$}* (our unpublished results), indicating that *cor^6* is partially dominant. On the basis of these results, we conclude that the *cor^6* allele has antimorphic functions.

Defects in coracle Mutant Embryonic and Imaginal Epithelial Cells

Several studies have suggested that *coracle* and some of the other genes required for dorsal closure may play a role in epithelial morphogenesis (reviewed in Noselli, 1998). To better assess the functions of *coracle* in the embryonic epidermis, we have examined phenotypes of null and strongly hypomorphic mutant embryos. Cuticle preparations of *coracle* mutant embryos display characteristic epidermal phenotypes in addition to dorsal closure defects. In *coracle* mutant embryos the cuticle appears to be thinner than normal and often appears to split into two layers in cuticle preparations (Figure 1, B, D, I, and J). The cuticular thinning is most obvious on the ventral surface where the denticle belts appear faint in cuticle preparations. Although the overall segmental pattern is normal, denticle belts contain fewer than normal denticles (Figure 1, E and F), and there are correspondingly fewer hairs on the dorsal side. Ultrastructural examination of the epidermis and cuticle reveals that the apparent delamination of the cuticle results from a failure of the epicuticle to adhere to the procuticle (Figure 1, I and J). All of

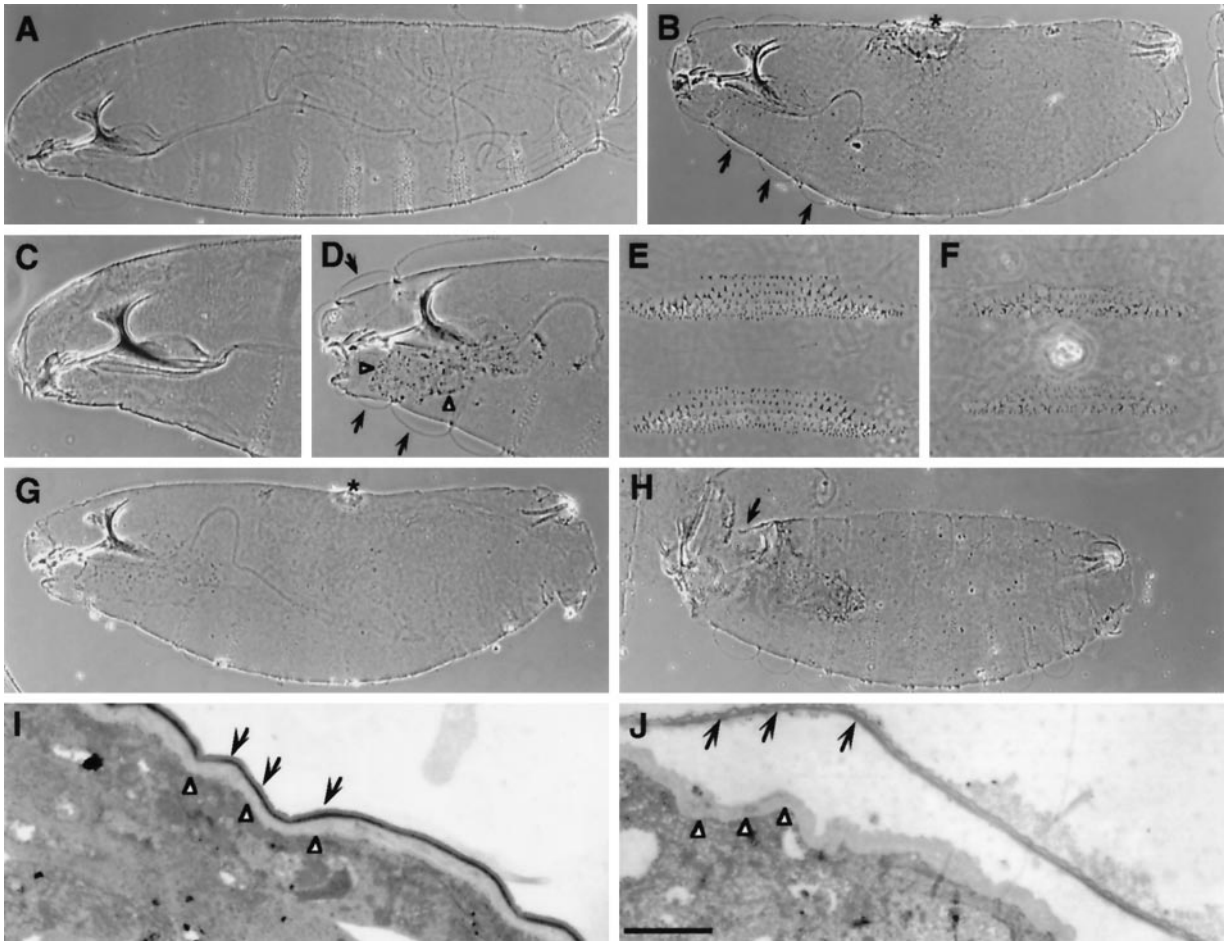

Figure 1. Cuticular phenotypes of *coracle* mutant embryos. Phase-contrast photomicrographs of wild-type (A, C, and E) and *coracle* mutant embryos (B, D, and F). (A) Wild-type embryonic cuticular pattern, lateral view. (B) A similarly oriented $cor^5/Df(2)cor^{P97}$ embryo demonstrating the characteristic dorsal hole (*) and detached cuticle (arrows) phenotypes. (C and D) The anterior ends of wild-type and $cor^2/Df(2)cor^{P97}$ mutant embryos, respectively. Delaminated cuticle (arrows) in the *coracle* mutant embryo is obvious in the naked area of each segment. In addition, the necrotic remains of the salivary glands characteristic of *coracle* mutant embryos are apparent (arrowhead). (E and F) High-magnification views of the ventral denticle belts from the third and fourth abdominal segments in a wild-type (E) and a $cor^5/Df(2)cor^{P97}$ mutant embryo (F). Note that there are fewer denticles and that they are less distinctly formed in *coracle* mutants, although the overall pattern appears normal. (G and H) Differences between the phenotypes of $cor^6/Df(2)cor^{P97}$ (G) and cor^6/cor^6 (H). Although $cor^6/Df(2)cor^{P97}$ embryos show a typical severe *coracle* embryonic phenotype with a dorsal hole (*), cor^6/cor^6 embryos display a clear anterior–open phenotype (arrow) that is not observed in any of the other *coracle* alleles. (I and J) Transmission electron micrographs of the epidermis and cuticle of late stage 17 wild-type (I) and cor^5 (J) mutant embryos. Note that in the cor^5 mutant tissue the epicuticle (black arrows) has separated from the procuticle (white arrowheads). Bar (I and J), 1 μm.

the embryonic lethal alleles also display salivary gland defects, which are apparent as necrotic material that remains in cuticle preparations (Figure 1D). This salivary gland defect was observed in embryos that had been aged beyond the stage at which wild-type embryos hatch as larvae, suggesting that this necrosis is a very late effect.

The salivary glands have been shown previously to express *coracle* at high levels (Fehon *et al.*, 1994; Ward *et al.*, 1998). To study the effects of loss of *coracle* function at the cellular level in epithelial cells, we examined the morphology of salivary gland epithelia in cor^5 mutant embryos using several molecular markers for the plasma membrane. These experiments were performed in midembryogenesis (stage 14), before the salivary gland necrosis described earlier is apparent. Markers for the adherens junction (Armadillo, Figure 2, C and D, and Notch, Figure 2, E and F) and the apical membrane (Crumbs, Figure 2, G and H) all displayed normal subcellular localizations in cor^5 mutant cells. It is important to note that these embryos had no detectable Coracle protein and that *coracle* is not expressed maternally (Fehon *et al.*, 1994). These results indicate that the apical–basal polarity of epi-

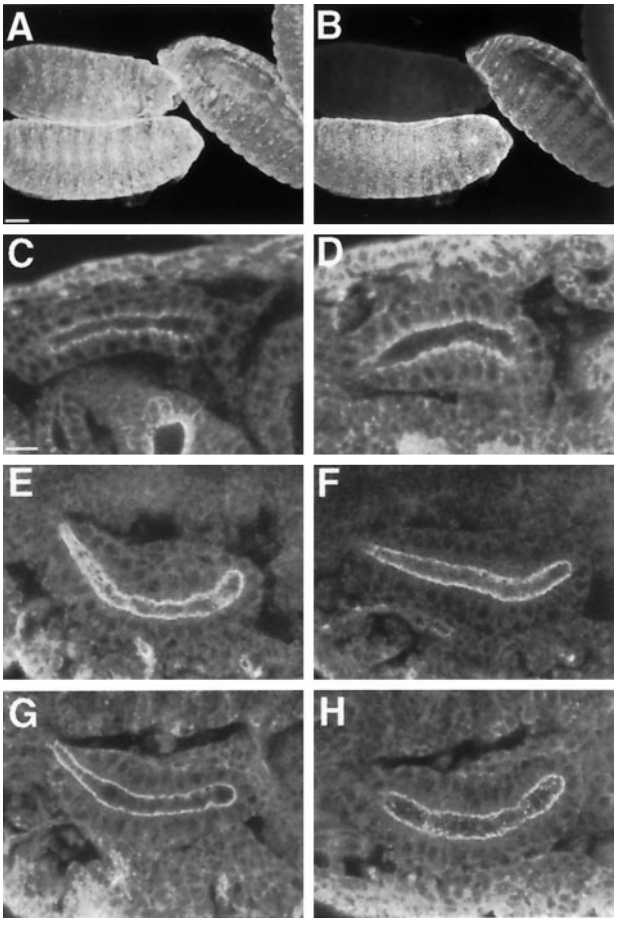

Figure 2. Apical–basal cellular polarity is normal in *coracle* null mutant embryos. (A and B) Confocal projections of a field of embryos double-labeled with anti–α-Spectrin (A) as a labeling control and anti-Coracle (B) to demonstrate that *cor*^{5} mutant embryos do not express detectable amounts of Coracle. (C–H) Wild-type (C, E, and G) and *cor*^{5} mutant (D, F, and H) stage 14 embryonic salivary glands stained with anti-Armadillo (C and D), anti-Notch (E and F), and anti-Crumbs (G and H) antisera. The subcellular localization of all three proteins is normal in *cor*^{5} mutant cells. Bars, 50 μm (A and B), 10 μm (C–H).

thelial cells is not grossly affected by loss of Coracle function.

Baumgartner *et al.* (1996) reported that strongly hypomorphic alleles of *Neurexin* lack pleated septate junctions in ectodermal epithelia and display transepithelial barrier defects (Baumgartner *et al.*, 1996). We reported recently (Ward *et al.*, 1998) that in *cor*^{5} mutant embryos, Neurexin is mislocalized, raising the possibility that the integrity of the septate junction is compromised in *coracle* mutant embryos. To investigate this idea, we conducted an ultrastructural examination of the epidermis and internal epithelia of late stage 17 mutant embryos. Similar to the observations regarding loss of *Neurexin*, we found that the septate junction in *cor*^{5} mutant epithelia was disrupted. Although the adherens junction appeared unaffected, the individual septae that characterize the pleated septate junction were always absent in *cor*^{5} mutant tissue (Figure 3, compare A with B). We occasionally observed electron-dense material in the intermembranal space, but this material was not organized into an array of discrete septae.

To examine the functional consequences of this lack of an organized septate junction, we tested the transepithelial barrier function of *coracle* mutant epithelia using a 10-kDa rhodamine-labeled dextran. We injected this dye into the hemocoel of stage 16 embryos. Although in wild-type embryos the dextran was confined to the hemocoel even 1 h after injection, in *cor*^{5} mutant embryos the dextran rapidly crossed the salivary gland epithelium and filled the luminal space (Figure 3F). The epidermis, hindgut, and trachea were similarly compromised. Taken together, these results demonstrate the essential requirement for *coracle* in the integrity of the transepithelial barrier function of the septate junction.

To examine further the effects of loss of *coracle* function in epithelial cells, we used somatic mosaic analysis to generate *cor*$^-$ cells in the imaginal epithelium. *cor*^{4} somatic clones were generated ~76 h after egg laying using the FLP recombinase/FRT target system (Xu and Rubin, 1993). *coracle* mutant clones were observed in late third instar wing imaginal discs using anti-Coracle antibodies to identify mutant cells (Figure 4) (at least 10 clones were observed for each antiserum used). The *cor*^{4} allele was chosen for this analysis because it is a strong allele that disrupts the ability of Coracle to associate with the plasma membrane (Ward *et al.*, 1998). Cells within the mutant clones were contiguous with the rest of the imaginal epithelium and appeared normally shaped. As previously described for embryonic tissues, we observed that loss of *coracle* function in imaginal epithelial cells resulted in disruption of Neurexin localization (Figure 4, A–F). In

Figure 3 (facing page). The ultrastructure and transepithelial barrier function of the septate junction is disrupted in the embryonic epithelia of *coracle* mutant embryos. (A and B) Transmission electron micrographs of the apical junctional complex in the epidermis of late stage 17 wild-type (A) and *cor*^{5} mutant (B) embryos. Although the adherens junction appears normal in the *cor*^{5} mutant tissue (black arrows; compare B with A), the region of the septate junction lacks the individual septae that characterize the pleated septate junction in the wild-type tissue (region between the arrowheads in A). (C–F) The transepithelial barrier function of the septate junction is disrupted in *cor*^{5} mutant embryos. (C–F) Differential interference contrast micrographs (C and D) and confocal optical sections (E and F) of stage 16 wild-type (C and E) and *cor*^{5} mutant (D and F) embryos showing the diffusion of a 10-kDa rhodamine–dextran injected into the hemocoel. Note that in the wild-type embryo the dextran fails to cross the salivary gland epithelium (arrows), whereas in the mutant embryo the dextran crosses the salivary gland epithelium as well as the epidermis. Bars, 250 nm (A and B), 10 μm (C–F).

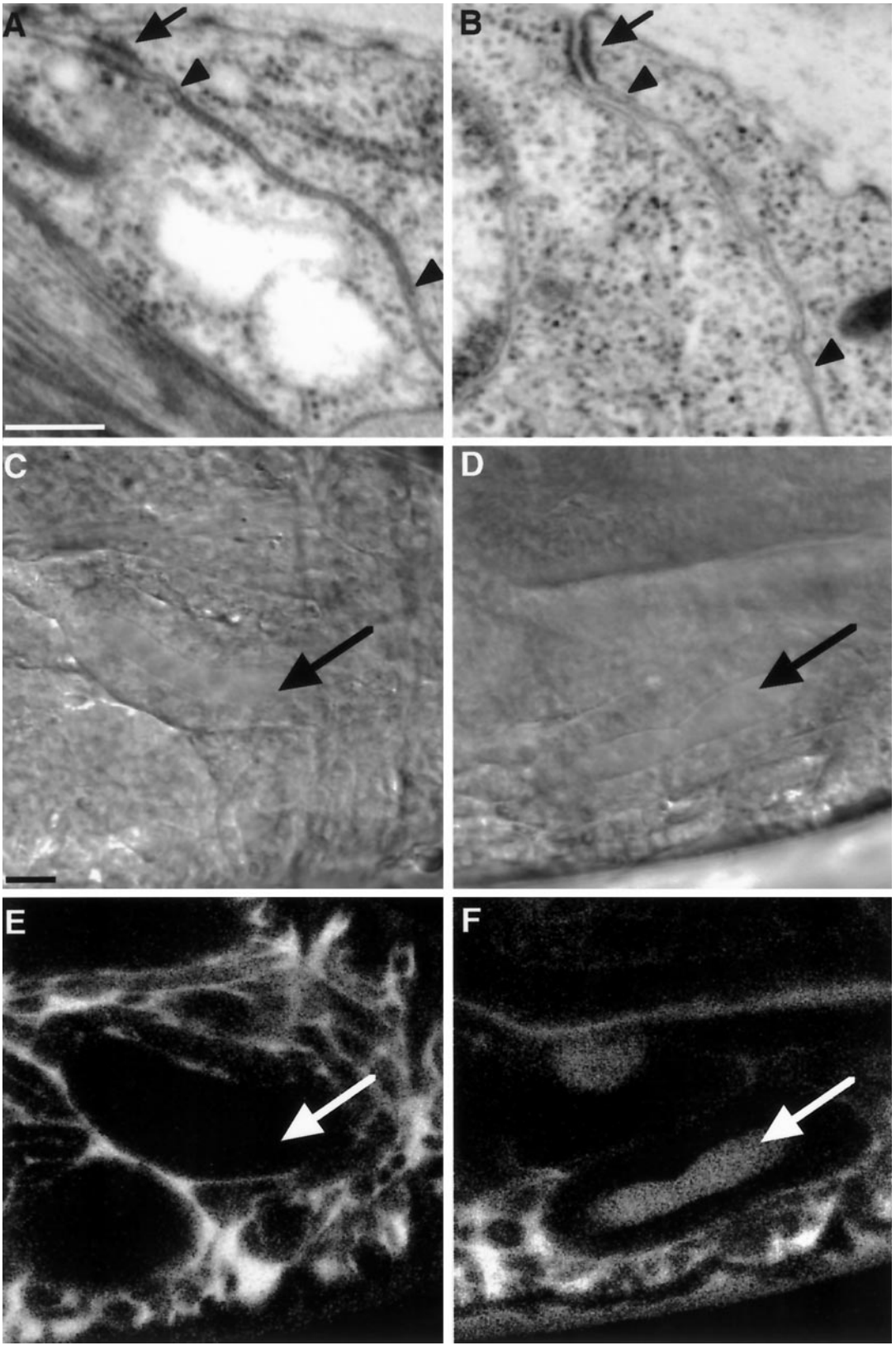

Figure 3.

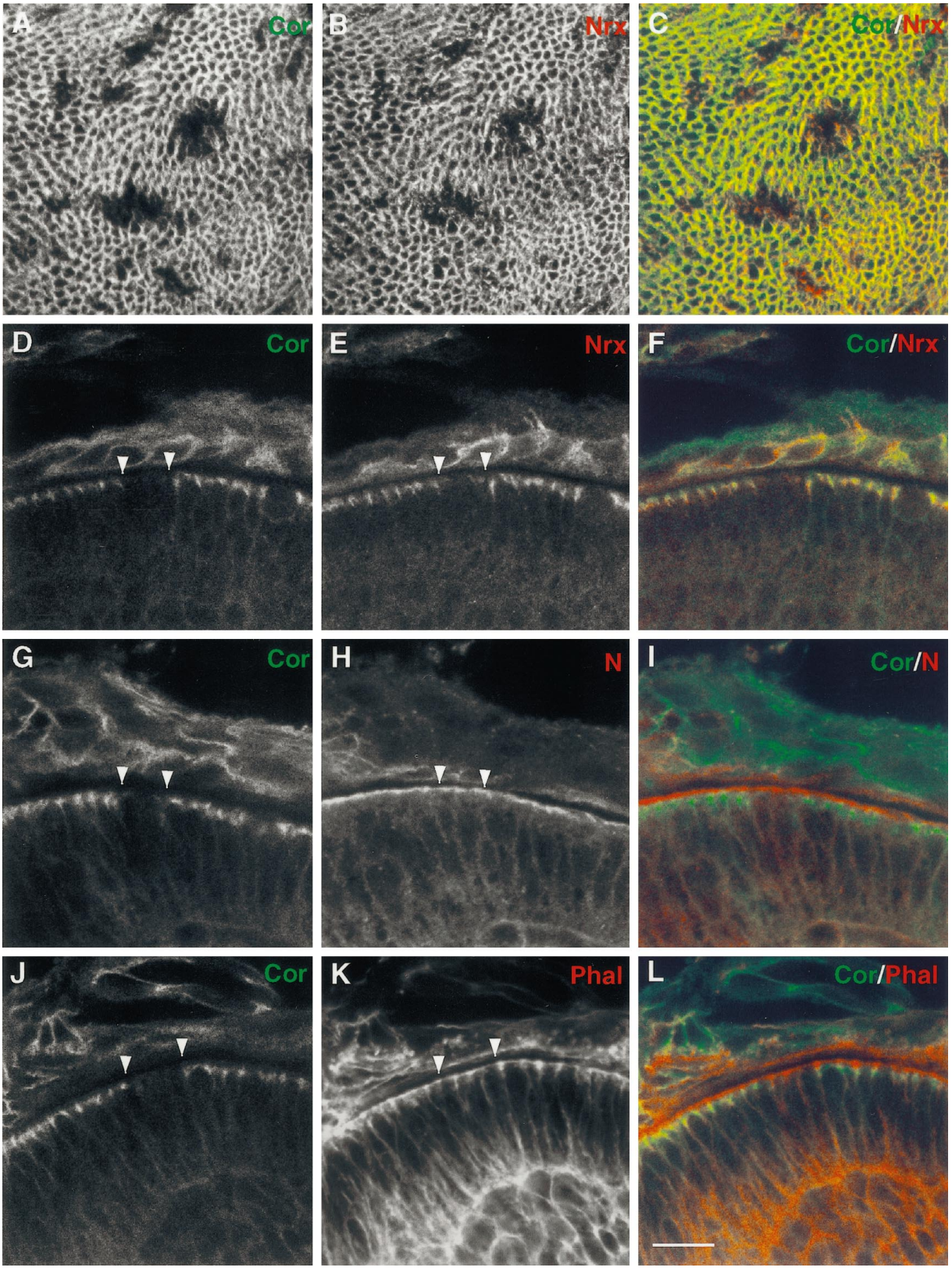
A
Cor
B
Nrx
C
Cor/Nrx
D
Cor
E
Nrx
F
Cor/Nrx
G
Cor
H
N
I
Cor/N
J
Cor
K
Phal
L
Cor/Phal

Figure 4.

addition, Neurexin protein was not readily detectable in the center of cor^- clones, suggesting that in imaginal epithelia Neurexin is not stable in the absence of *coracle* function. To assess apical–basal polarity and cytoskeletal organization in cor^- cells, we stained imaginal discs with antibodies for Notch (Figure 4, G–I), β_H-Spectrin, and Moesin (our unpublished results). As in the embryonic epidermis, these markers for the apical junctional region were localized normally in mutant cells. In addition, the distribution of filamentous actin was examined using rhodamine phalloidin and was also found to be normal (Figure 4, J–L). These results indicate that *coracle* function is not necessary for overall apical–basal polarity or cytoskeletal organization in imaginal tissues; however, when adult flies were examined for the presence of cor^- tissue, no mutant clones could be observed either in the eye (using a w^+ marker) or in the thorax (using a y^+ marker for bristles), indicating that cor^- cells do not persist to the adult stage (our unpublished results).

coracle *Postembryonic Phenotypes*

As shown above, the majority of *coracle* alleles are embryonic lethal; however, some weak alleles and several hypomorphic allelic combinations did produce adult escapers (Figure 6 and Table 1). For example, cor^7 was mostly embryonic lethal, but it produced 7% of expected viable, fertile adults and can be maintained as a homozygous stock at 25°C. cor^{14} was almost exclusively larval lethal, but 0.3% of the expected homozygous class survived to viable adults. cor^{15} was completely viable, with 100% of the expected homozygotes surviving to adulthood. All of the *coracle* alleles that produced adult escapers displayed a similar range of adult defects (see below), although the severity and penetrance of the phenotypes varied with genotype. All of these alleles were also cold sensitive (our unpublished results).

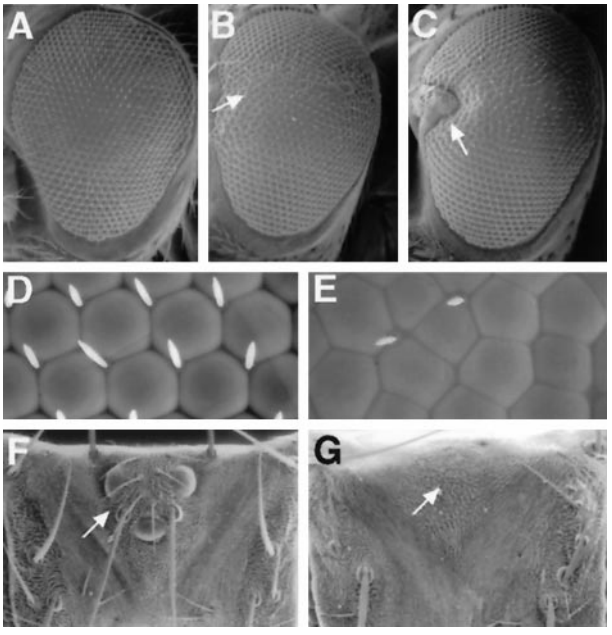

Figure 5. Eye and head defects associated with *coracle* hypomorphs. Scanning electron micrographs of adult eyes (A–E; anterior is to the left) and dorsal surface of heads (F and G). (A) cor^5/CyO (wild-type) eye showing normal morphology. (B) A cor^2/cor^{15} eye displays roughening across the equator (arrow). (C) In a cor^8/cor^{14} eye, an area of the eye has been replaced by head cuticle with associated bristles (arrow). (D) Higher-magnification view of a cor^5/CyO (wild-type) eye near the equator. Notice the regular hexagonal shape of the ommatidia and the precise spacing of the bristles. (E) Higher-magnification view of a cor^8/cor^{14} eye near the equator. Notice the irregularity in size and shape of the ommatidia and scarcity and misplacement of the bristles. (F) A dorsal view of a cor^5/CyO (wild-type) head showing the normal arrangement of three ocelli and associated bristles. (G) A dorsal view of a cor^4/cor^{15} head missing the ocelli and all associated bristles.

All *coracle* escapers display some degree of a rough eye phenotype. These eye defects ranged from a slight roughening of the eye, especially across the equator (Figure 5B), to eyes in which part of the eye tissue in the anterior equatorial region was replaced by head cuticle (Figure 5C). The penetrance of severe phenotypes increased with the strength of the *coracle* allele, to include up to 60% of the mutant adults. Histological sections show that the roughened appearance of *coracle* mutant eyes was caused by abnormally shaped, fused, improperly spaced, and occasionally misoriented ommatidia, rather than abnormal photoreceptor cell differentiation (our unpublished results). Essentially all of the ommatidia in the mutant eyes displayed normal numbers and positions of photoreceptors. Interommatidial bristles were also frequently lost in the roughened area (Figure 5E). Another very penetrant phenotype seen in *coracle* mutant animals was partial or total loss of the ocelli and associated bristles (Figure 5, compare G with F).

Figure 4 (facing page). Neurexin is affected but apical–basal polarity is normal in imaginal cells lacking *coracle* function. (A–L) Confocal micrographs of clones of cor^4 cells that were induced at ~76 h of development (early third instar) using the FLP/FRT system. A, D, G, and J display Coracle staining, B and E display Nrx staining, H displays Notch staining, and K displays filamentous actin stained with rhodamine–phalloidin. C, F, I, and L show merged images. (A–C) Projections of tangential optical sections through the apical portion of a wing imaginal disk that has been stained with anti-Coracle (A) and anti-Neurexin (B) antibodies. Note in B that in the absence of Coracle, Neurexin staining is also diminished. (D–L) Optical cross sections of the wing imaginal epithelium stained for Nrx and other apical membrane markers. Loss of Nrx staining in cor^4 cells is also apparent in cross section (E; arrowheads mark borders of the clone), whereas staining for Notch (H), an apically localized transmembrane protein, and filamentous actin (K), which is concentrated in the apical junctional region, appear to be unaffected. Bar, 10 μm.

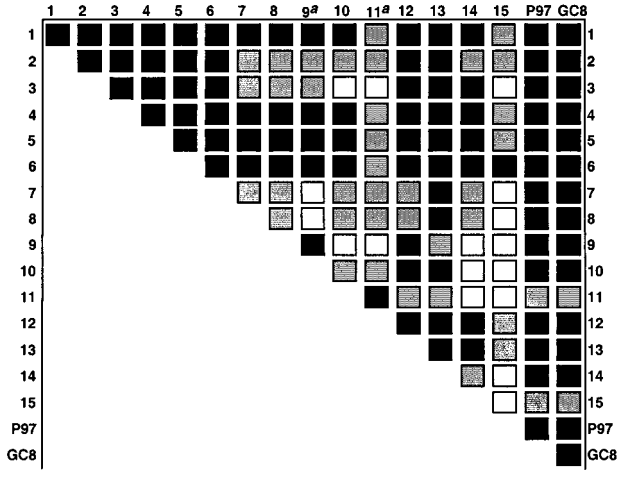

Figure 6. Complementation analysis of *coracle* alleles. Animals heterozygous for *coracle* alleles were crossed, and the percentage of expected cor^{y}/cor^{x} animals was calculated. Homozygous mutant phenotypes are indicated along the diagonal. Black indicates that the allelic combination was lethal, gray indicates that <75% of the expected progeny survive, and white indicates that 75% or more of the expected animals survive to adults. Note: *a*, not rescuable with *P{Up-cor*$^{+}$*}*; P97, *Df(2R)cor*^{P97}; GC8, *Df(2R)enb*^{GC8}.

In addition to the eye defects, *coracle* hypomorphic escapers displayed a range of other pleiotropic defects. These included wing vein phenotypes (interrupted cross veins and truncated fifth veins), rotational defects in the male genital apparatus, kinked or curved bristles, and leg abnormalities. Also both male and female escapers displayed partial or complete sterility (our unpublished results).

Complementation Analysis

To better examine the genetic function of the *coracle* alleles, and to determine whether *coracle* has genetically separable functional domains, we performed pairwise complementation analysis between all of the *coracle* alleles and two deficiencies that uncover the locus. This analysis revealed some cases of partial complementation in combinations of lethal with viable alleles (Figure 6). In addition, some alleles displayed antimorphic properties.

The behavior of alleles in the complementation analysis did not always correspond to allelic strength as determined by embryonic phenotype. Although strong *coracle* alleles displayed similar phenotypes when in *trans* with the deficiencies (Table 1), they did not behave similarly when in *trans* with weaker alleles (Figure 6). For example, although cor^{4} and cor^{5} were lethal when in *trans* with weak alleles, cor^{3}, another allele with a strong embryonic phenotype, almost fully complemented cor^{10} and cor^{11}. cor^{3} also partially complemented several other alleles (cor^{7}–cor^{9}; Figure 6). In addition, cor^{2} partially complemented some weaker alleles (cor^{7}–cor^{10}, cor^{14}; Figure 6), although it displayed a strong embryonic phenotype (Table 1). These results imply that there may be more than one functional domain within Coracle, and that mutations that disturb one functional domain can complement mutations that disrupt another.

Two other alleles, cor^{1} and cor^{6}, displayed characteristics that were not expected from the embryonic phenotypic analysis. cor^{1}, an allele that displayed an intermediate embryonic phenotype (Table 1), produced phenotypes similar to those of the strong alleles cor^{4} and cor^{5} when in *trans* with weaker coracle alleles (Figure 6). cor^{6}, an allele that displayed a strong embryonic phenotype in combination with deficiencies (Table 1) and an anterior open phenotype when homozygous (Figure 1H), was unusual in that it failed to even partially complement cor^{15} (Figure 6). cor^{15}, a weak allele (Table 1), was semiviable even in combination with deficiencies of the *coracle* locus and only displayed completely penetrant lethality in combination with cor^{6}. These results suggest that cor^{1} and cor^{6} encode mutant proteins that have antimorphic functions and therefore interfere with residual *coracle* function encoded by weaker alleles such as cor^{15}.

cor^{7}, an intermediate allele based on homozygous embryonic phenotype (Table 1), was partially viable and complemented most weak alleles, although other intermediate alleles (for example, cor^{12}) did not (Figure 6). In addition, two alleles, cor^{9} and cor^{11}, were homozygous lethal with no adult escapers, but they were viable or semiviable with several weak alleles in the complementation analysis (Figure 6); however, neither of these alleles could be rescued by *P{Up-cor*$^{+}$*}* (Table 1). This suggested either that these two mutations were not allelic to *coracle*, or that second-site lethals were associated with them. To determine which of these possibilities was true, the two alleles, along with the cor^{2} allele as a control, were mapped by recombination with a P-element, *P{white-un3}AA48*, that has been cytologically mapped to 56B, near the cytological position of *coracle* at 56C. All three alleles mapped within 1 cm of *P{white-un3}AA48*, indicating that cor^{9} and cor^{11} are allelic to *coracle*.

coracle *Genetic Interactions with* **Egfr^{Elp}**

Two *coracle* alleles have been shown previously to effectively suppress the hypermorphic $Egfr^{Elp}$ mutation in a dominant manner (Fehon *et al.*, 1994). $Egfr^{Elp}$ causes a roughening and a reduction in size of the *Drosophila* eye due to increased entry into S-phase and subsequent cell death (Baker and Rubin, 1992). To determine whether $Egfr^{Elp}$ suppression by *coracle* is allele specific or is instead directly proportional to the level of *coracle* function, we examined the ability of the new *coracle* alleles to suppress the eye phenotype of

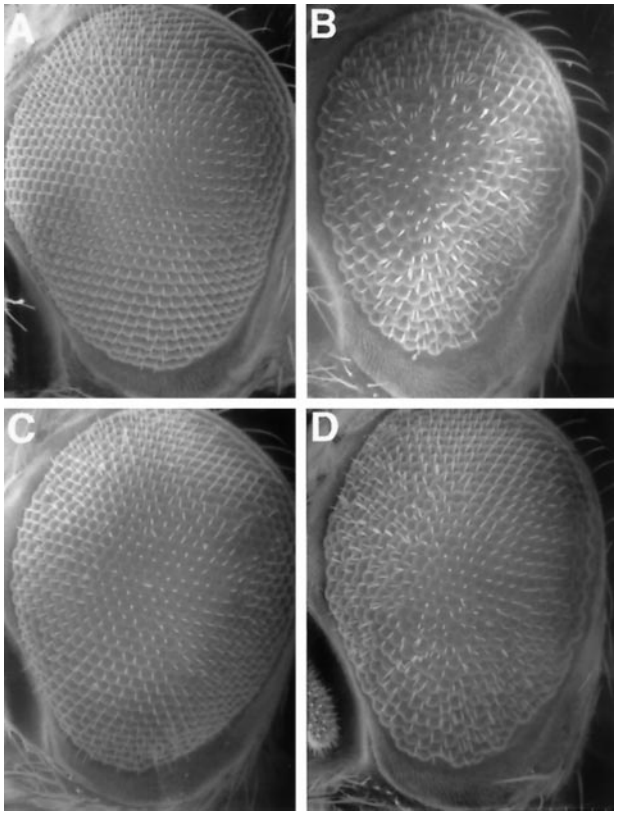

Figure 7. Genetic interactions between *coracle* and *Egfr*. Scanning electron micrographs of adult eyes. Anterior is to the left. (A) A cor^5/CyO (wild-type) eye and a $Egfr^{Elp}/CyO$ eye (B) that displays the dominant rough eye phenotype. (C) A $cor^{12}/Egfr^{Elp}$ eye showing full suppression of the $Egfr^{Elp}$ rough eye phenotype. (D) A $cor^5/Egfr^{Elp}$ eye that displays moderate roughness.

$Egfr^{Elp}$ (Table 1). Interestingly, the ability to suppress $Egfr^{Elp}$ does not correlate strictly with phenotypic strength of *coracle* alleles. The two deficiencies that uncover the *coracle* locus (our unpublished results) and the null allele cor^5 (Figure 7D and Table 1) only partially suppress the $Egfr^{Elp}$ eye phenotype, less efficiently than does either cor^1 or cor^2 (Fehon *et al.*, 1994). In addition, an intermediate and a weak *coracle* allele, cor^{12} and cor^{15}, respectively, are the strongest suppressors of $Egfr^{Elp}$ (Figure 7C and Table 1). These results indicate that the $cor/Egfr^{Elp}$ interaction is not strictly dose sensitive, and instead suggest that some mutant Coracle proteins may interact with the EGFR pathway in an allele-specific manner.

DISCUSSION

Previous analyses have shown that *coracle* is required during the process of dorsal closure and that it interacts genetically with hypermorphic mutations at the *Egfr* locus (Fehon *et al.*, 1994), but they have not examined the role of this conserved junctional protein in epithelial structure, morphogenesis, or apical–basal polarity. Here we have characterized the null phenotype of *coracle* mutations in embryos and in somatic mosaic clones of mutant cells. We show that although cells lacking *coracle* function display septate junction defects at the ultrastructural level and disruption of the transepithelial barrier, *coracle* mutations do not appear to affect apical–basal polarity or structural integrity of epithelial cells. Nonetheless, embryonic epithelia display a range of defects in *coracle* mutant animals that may result from disruption of an apical–basal barrier function that is dependent on *coracle* function. Data from somatic mosaic and genetic complementation analyses indicate that *coracle* functions throughout development of the imaginal epithelia and is necessary for differentiation of adult structures. Furthermore, complementation analysis suggests that the conserved amino terminal region (CNTR) of Coracle constitutes a functional domain and that sequences C-terminal to this domain may also be functionally significant.

Functional Domains within Coracle

In vitro studies of Protein 4.1, Coracle, and related family members indicate that the conserved N-terminal ~300 aa region forms a discrete functional domain that interacts with the cytoplasmic tail of a transmembrane partner (Rees *et al.*, 1990; Ward *et al.*, 1998). In most family members, there is also at least one other functional domain within the protein (Rees *et al.*, 1990; McCartney and Fehon, 1997). In the case of erythrocyte Protein 4.1, the second domain is known to bind to spectrin and actin, thereby linking the membrane to the cytoskeleton (Correas *et al.*, 1986).

The complementation analysis described here provides a powerful tool for examining the functional organization of *coracle*. For example, nonsense or missense mutations that inactivate one functional domain should behave in an antimorphic or "dominant negative" manner because they interfere with wild-type protein by competing for binding to an interacting partner in a nonproductive manner. Of particular interest in this regard are the cor^1 and cor^2 mutations, because we have shown previously that both alleles result from nonsense mutations just 3′ to the CNTR (Fehon *et al.*, 1994). Consistent with the notion that the CNTR encodes a functional domain (Ward *et al.*, 1998), we find that cor^1 displays an antimorphic phenotype in combination with hypomorphic *coracle* alleles (Figure 6). Furthermore, the fact that cor^1 is expressed at greater levels than cor^2 (Fehon *et al.*, 1994) suggests that although cor^2 should have a more severe embryonic phenotype, cor^1 would have more severe antimorphic phenotypes, as we have observed. Additionally, we find that cor^6, a missense mutation that

disrupts the function of the CNTR (Ward *et al.*, 1998), has antimorphic properties. These results also imply that Coracle sequences C-terminal to the CNTR constitute a separate functional domain.

If these alleles have antimorphic functions, then one might expect them to have dominant phenotypes in heterozygotes. Indeed, we have observed partially dominant lethality in flies heterozygous for the cor^6 mutation that can be suppressed by adding an additional dose of cor^+. However, given the high endogenous level of *coracle* expression in wild-type individuals and the relatively low levels of expression of cor^1 and cor^6 protein that have been observed (Fehon *et al.*, 1994; Ward *et al.*, 1998), it is not surprising that dominant antimorphic phenotypes are not readily observed in heterozygous flies. An antimorphic effect is more readily observed, however, when cor^1 or cor^6 is in *trans* with a hypomorphic allele that produces less functional *coracle* product (Figure 6). Thus, the hypomorphic *coracle* alleles we have isolated can be used as a "sensitized" system to detect antimorphic *coracle* products or potentially to identify other genes that function together with *coracle* at the septate junction.

Although we did not observe instances of two strong *coracle* alleles complementing one another to produce viable adults, there were several instances of partial interallelic complementation between strong and weak alleles. For example, cor^3, which has a strong embryonic phenotype, appears to partially complement several of the weak alleles, whereas the other strong alleles do not (Figure 6). Interallelic complementation can be characteristic of mutations in proteins that interact with one another to form complexes (Clifford and Schüpbach, 1994). Although there are currently no biochemical data to indicate such an interaction for Coracle or Protein 4.1, there is evidence that other family members form dimeric complexes that are essential for normal function (Gary and Bretscher, 1993; Berryman *et al.*, 1995). The genetic results presented here suggest that self interactions are also possible in Coracle and that additional biochemical experiments to test for possible interactions should be performed.

coracle Cellular Functions

Previous studies have suggested that septate junctions perform various functions within epithelial cells, including mediating cell–cell adhesion, promoting intercellular interactions (especially those related to cell proliferation), maintaining a diffusional barrier between the apical and basolateral surfaces of an epithelial sheet (the so called "gate" function), and maintaining a barrier within the plane of the plasma membrane to prevent diffusion of lipids and membrane-bound proteins between the apical and basolateral membrane domains (the "fence" function) (Noirot-Timothée and Noirot, 1980; Wood, 1990; Mandel *et al.*, 1993; Woods and Bryant, 1993). Because Coracle is tightly associated with the septate junction and interacts directly with Neurexin, another component of the septate junction (Ward *et al.*, 1998), we examined the effect of loss of *coracle* function on septate junction morphology, epithelial integrity, and apical–basal polarity within the membrane. Ultrastructural analysis shows that the normally pleated appearance of septate junctions in the embryonic epidermis is lost in embryos that lack *coracle* function (Figure 3B). This result is similar to that previously reported for *Nrx* mutations and is consistent with our recent finding that *coracle* function is required for the maintenance of Neurexin localization (Ward *et al.*, 1998). Thus *coracle* function is necessary at the cytoplasmic face of the septate junction to localize Neurexin and possibly other proteins in the region of this intercellular junction that together function to form the pleated arrays that are characteristic of this structure.

Given this clear disruption of septate junction morphology, one might expect that many of the functions of this intercellular junction would also be perturbed by *coracle* mutations. Previous studies of the *dlg* gene, which encodes a PDZ (PSD-90, DLG, ZO-1)-repeat-containing protein that localizes to the septate junction in epithelial cells (Woods and Bryant, 1989), have demonstrated that *dlg* mutations display disruptions in apical–basal polarity and loss of epithelial organization (Abbott and Natzle, 1992; Woods *et al.*, 1997); however, examination of markers for apical–basal polarity in embryonic and imaginal epithelia that lack *coracle* function shows no general effect on epithelial polarity (Figures 2 and 4). Thus *coracle* and indeed the pleated structure of the septate junction do not appear necessary for the fence function of septate junctions that separates the apical and basolateral membrane domains. In addition, although the characteristic pleated structure that appears to link adjacent cells is missing in these mutations, the integrity of embryonic and imaginal epithelia is unaffected (Figures 2 and 4), indicating that these structures also do not play an essential role in maintaining epithelial cell adhesion. Thus, by these morphological and molecular criteria *coracle* does not appear necessary for overall epithelial structure, either within an individual cell or within a sheet of cells.

Despite the absence of gross morphological defects, we do consistently see defects in epithelial differentiation of *coracle* mutant cells. In the embryo, we have found that there is a morphological defect in the cuticle secreted by the apical ends of epithelial cells that is manifested by a delamination between the epicuticle and procuticle layers (Figure 1J). At the light level, we also have observed that the cuticle produced in *coracle* mutant embryos appears thinner than in wild-type embryos, suggesting that the overall ability to synthe-

size or deposit cuticle is affected in these embryos (Figure 1). In addition, we have observed necrosis of the salivary gland epithelium (Figure 1D) (Ward *et al.*, 1998). To our knowledge similar phenotypes have not been reported previously for other genes, although we have seen similar defects at the light level in *Nrx* mutant embryos (our unpublished results). Our experiments testing diffusion of fluorescent dextran molecules across embryonic epithelia indicate that Coracle is required for the gate function of the septate junction (Figure 3F), and a similar phenotype has been noted for *Nrx* mutations (Baumgartner *et al.*, 1996). It is possible that the cuticular defects observed in both mutations are due to disruption of the ability of the embryonic epithelia to produce an effective barrier to diffusion between the apical and basolateral cell surfaces. This barrier may be important to maintain a particular microenvironment at the apical end of cells that is necessary for proper cuticular deposition.

Another phenotype that is shared by *coracle* and *Nrx* mutations is the disruption of the process of dorsal closure, a coordinated series of cell shape changes and rearrangements that occurs midway through embryogenesis (Young *et al.*, 1993). Given the absence of gross epithelial defects in *coracle* mutant embryos or in mutant clones of cells in imaginal epithelia, it seems unlikely that the failure in dorsal closure is due to disruption of epithelial integrity, although it could represent a defect in the ability to modulate junctional contacts. Alternatively, it is possible that the transepithelial barrier that becomes established by the formation of septate junctions in the embryonic epithelium at the onset of dorsal closure is itself required for the process of dorsal closure to proceed properly. For example, signaling events during dorsal closure that are mediated by the product of the *decapentaplegic* gene, a secreted TGF-β–like peptide (Noselli, 1998), may require a unique apical environment to function effectively.

In imaginal tissues, *coracle* mutant cells are morphologically normal but fail to produce adult cuticular structures. This result could indicate that *coracle* mutant cells are incapable of differentiating adult cuticular structures, but this seems unlikely given that embryonic epithelial cells do differentiate in the absence of *coracle* function and that we find no evidence of cuticular scars from mutant clones in adults. Alternatively, this failure could represent an earlier loss of *coracle* mutant cells from the imaginal epithelium. One potential mechanism for this loss is cell competition, a well documented phenomenon in which cells that are at a proliferation disadvantage are lost from the imaginal epithelia (Simpson, 1979, 1981). This possibility is made more likely by the previous observation that *coracle* mutations suppress hypermorphic mutations in *Egfr* (see RESULTS) (Fehon *et al.*, 1994), suggesting that Coracle may function together with this receptor to promote cell proliferation in imaginal tissues.

Implications for the 4.1 Superfamily

The experiments presented here provide insights into the in vivo functions of *coracle*, a *Drosophila* member of the Protein 4.1 superfamily. Although erythrocyte Protein 4.1 and other family members generally have been considered to play a structural role in linking transmembrane proteins to proteins in the cytoplasm (Rees *et al.*, 1990), recently there has been increasing evidence that these proteins function in mediating intercellular signals. In particular, studies of the ERM proteins indicate that they play essential roles in mediating Rho-dependent signaling mechanisms that may function in the regulation of cell shape or establishment of cell–cell contacts (Hirao *et al.*, 1996). In addition, the product of the *NF2* gene, Merlin, is involved in regulating cell proliferation, although the mechanism by which this occurs is not yet understood (Trofatter *et al.*, 1993; Lutchman and Rouleau, 1996). Other family members, such as the protein tyrosine phosphatases, also are likely to function in cell–cell signaling, although their precise functions are also unknown (Banville *et al.*, 1994).

Genetic studies of *coracle* and other Protein 4.1 family members in *Drosophila* provide a powerful method for examining the in vivo functions of these proteins. Our data indicate that *coracle* is not necessary for overall maintenance of cell structure and apical–basal polarity or integrity of the actin cytoskeleton, as might have been assumed from previous studies of Protein 4.1 function in erythrocytes. Instead, the data presented here indicate that *coracle* is required for establishment of a transepithelial barrier provided by septate junctions. Although this function is likely to be important to all epithelial cells, it is currently unclear whether this cellular defect alone can explain all of the phenotypes that we observe in flies that carry *coracle* mutations. Further genetic and molecular–genetic studies of *coracle* and related family members in *Drosophila*, such as *Merlin* and *Moesin* (McCartney and Fehon, 1996), should continue to provide new insights into the functions of this family of membrane-associated proteins.

ACKNOWLEDGMENTS

We thank R. Murray and C. Campbell for technical assistance, L. Eibest for help with the scanning electron microscopy, S. Ward for assistance with the transmission electron microscopy, the Rubin lab and the Indiana stock center for fly stocks, M. Peifer, D. Kiehart, E. Knust, and G. Thomas for providing antibodies, and our colleagues in the Fehon lab for valuable suggestions and discussions. R.S.L. was supported by a National Institutes of Health training grant in cell and molecular biology (GM07184). R.E.W. was supported by a National Institutes of Health training grant in genetics (5T32 GM07754). This research was supported by grants from the National Science Foundation (IBN-92066555) and the American Cancer Society (DB-84846) to R.G.F.

REFERENCES

Abbott, L.A., and Natzle, J.E. (1992). Epithelial polarity and cell separation in the neoplastic *l(1)dlg-1* mutant of *Drosophila*. Mech. Dev. *37*, 43–56.

Alloisio, N., Dalla Venezia, N., Rana, A., Andrabi, K., Texier, P., Gilsanz, F., Cartron, J.-P., Delaunay, J., and Chishti, A.H. (1993). Evidence that red blood cell protein p55 may participate in the skeleton-membrane linkage that involves protein 4.1 and glycophorin C. Blood *82*, 1323–1327.

Baker, N.E., and Rubin, G.M. (1992). Ellipse mutations in the *Drosophila* homologue of the EGF receptor affect pattern formation, cell division, and cell death in eye imaginal discs. Dev. Biol. *150*, 381–396.

Banville, D., Ahmad, S., Stocco, R., and Shen, S.H. (1994). A novel protein-tyrosine phosphatase with homology to both the cytoskeletal proteins of the band 4.1 family and junction-associated guanylate kinases. J. Biol. Chem. *269*, 22320–22327.

Baumgartner, S., Littleton, J.T., Broadie, K., Bhat, M.A., Harbecke, R., Lengyel, J.A., Chiquet-Ehrismann, R., Prokop, A., and Bellen, H.J. (1996). A *Drosophila* neurexin is required for septate junction and blood-nerve barrier formation and function. Cell *87*, 1059–1068.

Berryman, M., Gary, R., and Bretscher, A. (1995). Ezrin oligomers are major cytoskeletal components of placental microvilli: a proposal for their involvement in cortical morphogenesis. J. Cell Biol. *131*, 1231–1242.

Boedigheimer, M., Bryant, P., and Laughon, A. (1993). Expanded, a negative regulator of cell proliferation in *Drosophila*, shows homology to the NF2 tumor suppressor. Mech. Dev. *44*, 83–84.

Boedigheimer, M., and Laughon, A. (1993). expanded: a gene involved in the control of cell proliferation in imaginal discs. Development *118*, 1291–1301.

Clifford, R., and Schüpbach, T. (1994). Molecular analysis of the *Drosophila* EGF receptor homolog reveals that several genetically defined classes of alleles cluster in subdomains of the receptor protein. Genetics *137*, 531–550.

Conboy, J., Chasis, J., Winardi, R., Tchernia, G., Kan, Y., and Mohandas, N. (1993). An isoform-specific mutation in the protein 4.1 gene results in hereditary elliptocytosis and complete deficiency of protein 4.1 in erythrocytes but not in nonerythroid cells. J. Clin. Invest. *91*, 77–82.

Correas, I., Speicher, D.W., and Marchesi, V.T. (1986). Structure of the spectrin-actin binding site of erythrocyte protein 4.1. J. Biol. Chem. *261*, 13362–13366.

Diaz-Benjumea, F.J., and Garcia-Bellido, A. (1990). Behaviour of cells mutant for an *EGF receptor* homologue of *Drosophila* in genetic mosaics. Proc. R. Soc. Lond. B Biol. Sci. *242*, 36–44.

Fehon, R.G., Dawson, I.A., and Artavanis-Tsakonas, S. (1994). A *Drosophila* homologue of membrane-skeleton protein 4.1 is associated with septate junctions and is encoded by the *coracle* gene. Development *120*, 545–557.

Fehon, R.G., Johansen, K., Rebay, I., and Artavanis-Tsakonas, S. (1991). Complex cellular and subcellular regulation of Notch expression during embryonic and imaginal development of *Drosophila*: implications for Notch function. J. Cell Biol. *113*, 657–669.

Fehon, R.G., LaJeunesse, D., Lamb, R., McCartney, B.M., Schweizer, L., and Ward, R.E. (1997). Functional studies of the Protein 4.1 family of junctional proteins in *Drosophila*. Soc. Gen. Physiol. Ser. *52*, 149–159.

Gary, R., and Bretscher, A. (1993). Heterotypic and homotypic associations between ezrin and moesin, two putative membrane-cytoskeletal linking proteins. Proc. Natl. Acad. Sci. USA *90*, 10846–10850.

Giebelhaus, D.H., Eib, D.W., and Moon, R.T. (1988). Antisense RNA inhibits expression of membrane skeleton protein 4.1 during embryonic development of *Xenopus*. Cell *53*, 601–615.

Grigliatti, T. (1986). Mutagenesis. In: *Drosophila*: a practical approach, ed. D. Roberts, Oxford: IRL Press, 39–58.

Hirao, M., Sato, N., Kondo, T., Yonemura, S., Monden, M., Sasaki, T., Takai, Y., Tsukita, S., and Tsukita, S. (1996). Regulation mechanism of ERM (ezrin/radixin/moesin) protein/plasma membrane association: possible involvement of phosphatidylinositol turnover and Rho-dependent signaling pathway. J. Cell Biol. *135*, 37–51.

Konsolaki, M., and Schupbach, T. (1998). windbeutel, a gene required for dorsoventral patterning in *Drosophila*, encodes a protein that has homologies to vertebrate proteins of the endoplasmic reticulum. Genes Dev. *12*, 120–131.

Lue, R.A., Marfatia, S.M., Branton, D., and Chishti, A.H. (1994). Cloning and characterization of hdlg: the human homologue of the *Drosophila* discs large tumor suppressor binds to protein 4.1. Proc. Natl. Acad. Sci. USA *91*, 9818–9822.

Lutchman, M., and Rouleau, G.A. (1996). Neurofibromatosis type 2: a new mechanism of tumor suppression. Trends Neurosci. *19*, 373–377.

Mandel, L.J., Bacallao, R., and Zampighi, G. (1993). Uncoupling of the molecular "fence" and paracellular "gate" functions in epithelial tight junctions. Nature *361*, 552–555.

Martuza, R.L., and Eldridge, R. (1988). Neurofibromatosis 2 (bilateral acoustic neurofibromatosis). N. Engl. J. Med. *318*, 684–688.

McCartney, B.M., and Fehon, R.G. (1996). Distinct cellular and subcellular patterns of expression imply distinct functions for the *Drosophila* homologues of moesin and the neurofibromatosis 2 tumor suppressor, merlin. J. Cell Biol. *133*, 843–852.

McCartney, B.M., and Fehon, R.G. (1997). The ERM family of proteins and their roles in cell-cell interactions. In: Cytoskeletal-membrane interactions and signal transduction, ed. Cowin, P., and Klymkowsky M.W., Austin, TX: R.G. Landes Biocience, 200–210.

McClatchey, A.I., Saotome, I., Ramesh, V., Gusella, J.F., and Jacks, T. (1997). The *Nf2* tumor suppressor gene product is essential for extraembryonic development immediately prior to gastrulation. Genes Dev. *11*, 1253–1265.

Noirot-Timothée, C., and Noirot, C. (1980). Septate and scalariform junctions in arthropods. Int. Rev. Cytol. *63*, 97–140.

Noselli, S. (1998). JNK signaling and morphogenesis in *Drosophila*. Trends Genet. *14*, 33–38.

Ponting, C.P., Phillips, C., Davies, K.E., and Blake, D.J. (1997). PDZ domains: targeting signalling molecules to sub-membranous sites. Bioessays *19*, 469–479.

Rebay, I., Fehon, R.G., and Artavanis-Tsakonas, S. (1993). Specific truncations of *Drosophila* Notch define dominant activated and dominant negative forms of the receptor. Cell *74*, 319–329.

Rees, D.J.G., Ades, S.E., Singer, S.J., and Hynes, R.O. (1990). Sequence and domain structure of talin. Nature *347*, 685–689.

Rouleau, G.A., et al. (1993). Alteration in a new gene encoding a putative membrane-organizing protein causes neurofibromatosis type 2. Nature *363*, 515–521.

Rubin, G.M., and Spradling, A.C. (1982). Genetic transformation of *Drosophila* with transposable element vectors. Science *218*, 348–353.

Simpson, P. (1979). Parameters of cell competition in the compartments of the wing disc of *Drosophila*. Dev. Biol. *69*, 182–193.

Simpson, P. (1981). Growth and cell competition in *Drosophila*. J. Embryol. Exp. Morph. *65*(suppl), 77–88.

Szüts, D., Freeman, M., and Bienz, M. (1997). Antagonism between EGFR and Wingless signalling in the larval cuticle of *Drosophila*. Development *124*, 3209–3219.

Tepass, U., and Hartenstein, V. (1994). The development of cellular junctions in the *Drosophila* embryo. Dev. Biol. *161*, 563–596.

Trofatter, J.A., et al. (1993). A novel moesin-, ezrin-, radixin-like gene is a candidate for the neurofibromatosis 2 tumor suppressor. Cell *72*, 791–800.

Ward, R.E.I., Lamb, R.S., and Fehon, R.G. (1998). A conserved functional domain of *Drosophila* Coracle is required for localization at the septate junction and has membrane-organizing activity. J. Cell Biol. *140*, 1463–1473.

Wieschaus, E., Nüsslein-Volhard, C., and Jürgens, G. (1984). Mutations affecting the pattern of the larval cuticle in *Drosophila melanogaster*. III. Zygotic loci on the X-chromosome and fourth chromosome. Roux's Arch. Dev. Biol. *193*, 296–307.

Wood, R.L. (1990). The septate junction limits mobility of lipophilic markers in plasma membranes of *Hydra vulgaris* (*attenuata*). Cell Tissue Res. *259*, 61–66.

Woods, D.F., and Bryant, P.J. (1989). Molecular cloning of the lethal (1) discs large-1 oncogene of *Drosophila*. Dev. Biol. *134*, 222–235.

Woods, D.F., and Bryant, P.J. (1993). Apical junctions and cell signalling in epithelia. J Cell Sci *17*(suppl), 171–181.

Woods, D.F., Wu, J.W., and Bryant, P.J. (1997). Localization of proteins to the apico-lateral junctions of *Drosophila* epithelia. Dev. Genet. *20*, 111–118.

Xu, T., and Rubin, G. (1993). Analysis of genetic mosaics in developing and adult *Drosophila* tissues. Development *117*, 1223–1237.

Young, P.I., Richman, A.M., Ketchum, A.S., and Kiehart, D.P. (1993). Morphogenesis in *Drosophila* requires nonmuscle myosin heavy chain function. Genes Dev. *7*, 29–41.